

## Surface Melting of Neon and Argon Films: Profile of the Crystal-Melt Interface

Da-Ming Zhu and J. G. Dash

*Department of Physics, University of Washington, Seattle, Washington 98195*

(Received 24 November 1987)

Surface melting in Ne films evolves with thickness from logarithmic to power-law temperature dependence. The thin-film behavior appears to be due to the expected exponential decay of solid order. The variation with thickness of the melting entropy is examined to determine the profile of the crystal-melt interface. The interface width is approximately 6 layers in Ne and 4 in Ar.

PACS numbers: 68.35.Rh, 64.70.Dv, 68.45.Gd

Recent experiments on Pb crystals,<sup>1</sup> Pb films,<sup>2</sup> and adsorbed Ar films<sup>3</sup> support basic predictions of the theory of surface melting.<sup>4,5</sup> In both systems an equilibrium layer of the melt liquid wets the solid-vapor interface at temperatures below the triple point, and grows in thickness as  $T$  approaches  $T_i$ . In Pb the thickness  $L_l$  of the liquid grows as  $|\ln(T_i - T)|$ , while in Ar the increase follows a power law  $(T_i - T)^{-n}$ , with  $n \cong \frac{1}{3}$ . The  $T$  dependence is controlled by the nature of the effective interactions between the interfaces of the liquid layer. Logarithmic growth is a consequence of short-range interactions,<sup>4-6</sup> which can be ascribed in the case of Pb to exponential screening of charge fluctuations by the conduction electrons in the liquid.<sup>7</sup> Long-range interactions produce power-law growth; consistent with expectations for films composed of van der Waals molecules,<sup>5,6</sup> the exponent in Ar corresponds to unretarded dispersion forces. But surface melting in other molecular films does not resemble that in Ar: Recent studies of O<sub>2</sub>/graphite<sup>8</sup> and methane/MgO<sup>9</sup> show approximately logarithmic growth. It has been suggested<sup>8</sup> that the difference is related to the thickness: In the O<sub>2</sub> and methane films the thickness of liquid ranged from 1 to 4 molecular layers, whereas in Ar it was between 6 and 9.5. The explanation implies a crossover from logarithmic growth in thin films to a power law in thick films. This Letter reports measurements in Ne films exhibiting such a crossover. We also show that the variation of melting entropy with film thickness can provide a means for determining the profile of the solid-structure order parameter, and we apply the method to Ne and Ar. The results are compared with theoretical estimates and computer simulations of the crystal-melt interface width in simple molecular systems.<sup>10-13</sup>

The Ne measurements are based on calorimetry of adsorbed multilayer films, consisting of 24 samples between 1 and 25 layers thick, at temperatures extending on both sides of the triple point,  $T_i = 24.54$  K.<sup>14</sup> We used the same exfoliated foam graphite cell and cryostat as for Ar.<sup>3</sup> The characteristics of Ne are somewhat better than those of Ar for this type of study, since the background heat capacity of the empty cell is much smaller at its triple point than at the  $T_i$  of Ar (83.8 K). We determine

that no bulk nucleation occurred in the experimental range, the vapor pressures of the films being appreciably below bulk Ne vapor pressure<sup>14</sup> down to 20 K.

All of the samples thicker than 6 layers show heat-capacity anomalies near 24 K. Figure 1 displays the re-

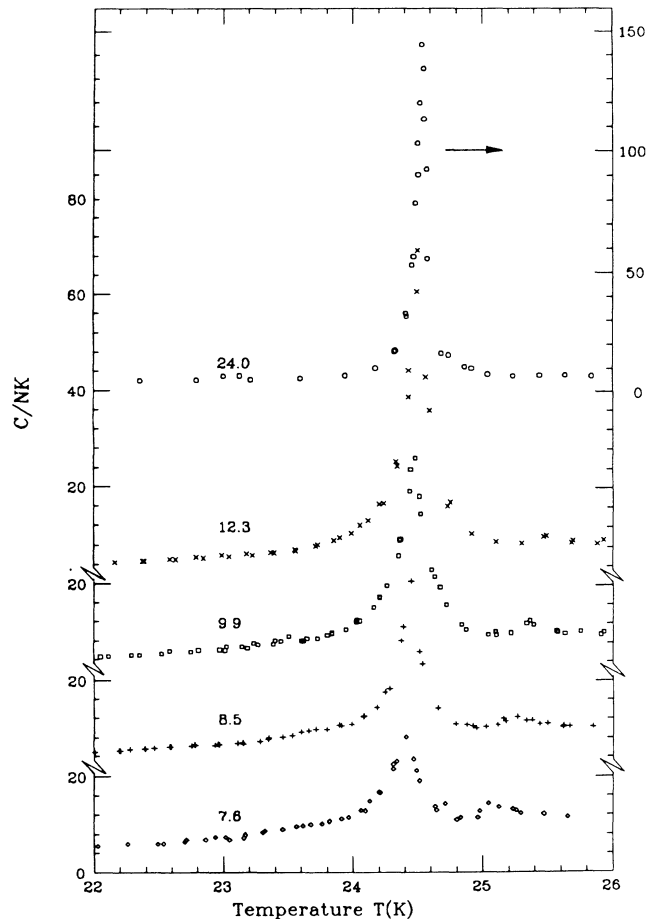


FIG. 1. Heat capacity of Ne films, showing melting anomalies near the triple point. The numbers are the film thicknesses in layers at 24.54 K. The rises, beginning well below the peaks, are due to surface melting. The small cusps at temperatures above the main peaks are caused by melting of substrate-field-compressed single layers next to the substrate.

sults obtained for several samples in this range, showing that peak height and sharpness increase with thickness, consistent with an approach to first-order melting in the bulk material. The rises begin well below the peaks, then steepen rapidly to maxima slightly below the bulk transition temperature. Small cusps at temperatures above the main peaks are identified as due to the melting of individual layers adjacent to the substrate, their higher melting temperatures being raised by the compression due to substrate attraction. Similar peaks were found in Ar films.<sup>3</sup>

During melting the total signal consists of terms due to the liquid and solid fractions and the progressive conversion from one to the other. In thick samples the phases are essentially homogeneous, except for portions close to the interfaces. If desorption, substrate-field, and interfacial effects are lumped in a correction  $\delta C$ , the heat capacity at constant total  $N$  is

$$C = Nc_s + N_l(c_l - c_s) + T\Delta s(dN_l/dT) + \delta C, \quad (1)$$

where  $N_l$ ,  $c_l$ , and  $c_s$  are the populations and specific heats of uniform phases and  $\Delta s$  is the melting entropy per molecule. The terms associated with melting are distinguishable from the rest by their temperature dependence, being functions of the difference  $\Delta T = (T_l - T)$ , while the remainder depends on  $T$  alone and is smooth except at  $T_l$ . Accordingly, melting signals for each sample near  $T_l$  were isolated by subtracting a slowly varying "background," approximated by a linear fit to the heat capacity over a region below the start of the precursor.

The conversion term in Eq. (1) dominates if  $N$  is not too large; estimates show that this holds in all the samples. If all other terms are negligible or can be subtracted away and if the surface melting follows the

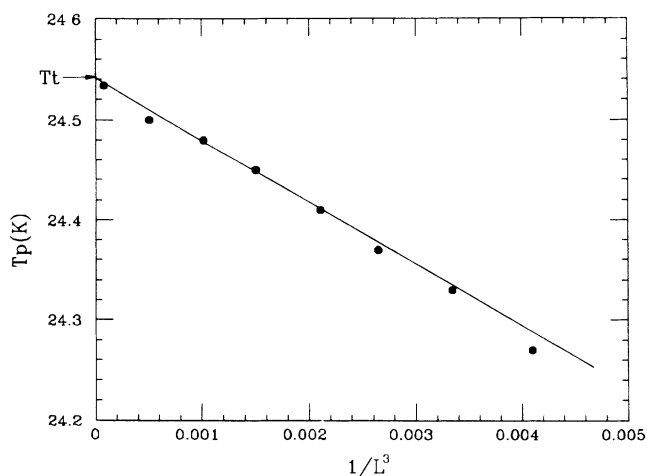


FIG. 2. Peak temperatures, showing the trend to higher temperature with increasing thickness. Proportionality to  $L^{-3}$  corresponds to surface melting controlled by long-range dispersion forces. The intercept is identified with the bulk triple-point temperature 24.541 K.

dispersion-force-dominated power law, the heat capacity will vary as  $\Delta T^{-4/3}$ , while melting governed by short-range interactions will vary as  $\Delta T^{-1}$ .

The determination of empirical exponents requires a precise thermometer calibration at  $T_l$ . This was obtained from the trend of the peak temperatures versus  $L$ , the total film thickness, as shown in Fig. 2. The linearity is a direct consequence of power-law growth in the thicker films. The growth of  $L_l$  in a film of arbitrary total  $L$  will follow the melting law of a semi-infinite solid, until the melting interface reaches the dense layers adjacent to the substrate, where the growth will slow and then cease. The termination causes the conversion term in the heat capacity to fall to zero, producing a peak at a temperature  $T_p < T_l$ . If the truncation is abrupt, the shift is related to  $L$  through the growth law. For thick molecular films one expects a power law with exponent  $\frac{1}{3}$ : In this range  $T_p$  should vary as

$$T_p = T_l - \text{const}/L^3. \quad (2)$$

Figure 2 shows that the shifts are linearly proportional to  $1/L^3$  at  $L > 10$ . (There should be a small curvature, unimportant in the thick region, because the thickness has not been corrected for the dense, unmelted layer.) The intercept is an *in situ* thermometer calibration, identified with the bulk transition  $T_l$ .

We analyzed the regions below the peaks to obtain average power-law exponents at  $7 < L < 24$ . The consistent fitting range extended over slightly more than one decade in reduced temperature,  $0.0055 < \Delta T/T_l < 0.075$ . Figure 3 shows that the average exponent changes with  $L$ , progressing from about 1 at  $L=7$  to  $\approx \frac{4}{3}$  at  $L=24$ . This trend is consistent with the expected crossover between short-range and long-range behavior.

In spite of the agreement, the test seems only a qualified success. The precision of the empirical exponents is not much better than the difference between

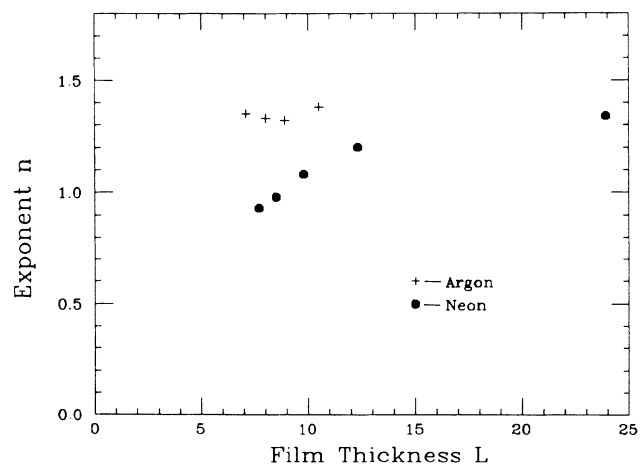


FIG. 3. Empirical power-law exponents of the heat capacity below the triple point, as functions of total film thickness.

the two theoretical values. The fitting range is limited because the exponents are not constant throughout the transition. It is desirable to relate the crossover to the physical properties of the system; furthermore, a basic assumption of the analysis, that of two sharply distinct phases, is incorrect. The analysis below avoids these deficiencies.

Theories and computer simulations of molecular systems predict a finite width of the crystal-melt interface, a gradation from bulk solid to bulk liquid properties extending over several atomic diameters.<sup>10-13</sup> Of particular relevance here, one expects a gradual change in the entropy density  $s(z)$  with distance  $z$  from the solid boundary. An approximation describes the gradation as an exponential attenuation of solidlike properties with distance from the solid boundary. More realistic calculations show that the change begins a short distance on the solid side of the boundary, so that the profile has a sigmoid shape in the central region, while the trend at greater distances on the liquid side is probably exponential: Some models approximate the entire range by a hyperbolic tangent.<sup>13,15</sup> The data can be described quite well by both the exponential and hyperbolic tangent functions, outlined below.

We first assume a simple exponential form; the entropy density  $s(z)$  varies with distance  $z$  from the solid as

$$s(z) = s_s + \Delta s(z) = s_s + \Delta s_m (1 - e^{-z/\xi'}), \quad (3)$$

where  $\Delta s_m$  is the transition entropy density of bulk phases and  $\xi'$  is the coherence length of the solid order parameter. We neglect the diffuseness of the liquid-vapor interface, a reasonable approximation if  $\xi'$  is much greater than the interface width, so that Eq. (3) with constant  $\xi'$  is assumed to extend throughout the liquid, to a sharp cutoff at the vapor boundary. The total transition entropy due to the melting of a finite thickness of film is an integral of  $\Delta s(z)$ ; with  $L'_0$  as a fitting parameter for the number of unmelted layers, the total entropy of melting  $L - L'_0$  layers is

$$\Delta S(L) = A\rho\Delta s_m \{L - L'_0 - \xi' [1 - \exp((L'_0 - L)/\xi')]\}, \quad (4)$$

where  $A$  is the area and  $\rho$  is the density of a liquid layer.  $L$  is known from the total thickness,  $A$  and  $\rho$  by vapor-pressure isotherms, and  $\Delta s_m$  by bulk measurements. With the two empirical parameters  $L'_0$  and  $\xi'$  Eq. (4) can be fitted to the data for both Ne and Ar, with standard deviations of about 8%. Slightly better fits can be made with a hyperbolic-tangent profile  $\Delta s(z) = \frac{1}{2} \Delta s_m [1 + \tanh(z/\xi)]$ . At  $z \gg \xi$ , the entropy density approaches the bulk liquid value as  $e^{-2z/\xi}$ , and so  $\xi/2$  is the effective coherence length at large distances.  $2\xi$  is the interface "width," the size of the central region where  $\Delta s$  undergoes its major change. Integration for  $\Delta s$  also requires a parameter, defined as  $L_0$ , to position the center of the interface relative to the substrate. The total transition entropy is

$$\Delta S(L) = A\rho\Delta s_m \left[ L - L_0 + \frac{1}{2} \xi \ln \left( \frac{1 + \exp[-2(L - L_0)/\xi]}{1 + \exp[-2L_0/\xi]} \right) \right]. \quad (5)$$

Figure 4 displays the experimental  $\Delta S(L)$  of Ne and Ar, with fitted curves according to Eq. (5). The best-fit parameters are, for Ne,  $\xi = 3$ ,  $L_0 = 6$ ; and for Ar,  $\xi = 1.9$ ,  $L_0 = 5$ . Standard deviations between the data and the fitted curves are 6% (Ne) and 7% (Ar). We also show the bulk entropy<sup>14</sup> for the same thickness range, i.e., how  $\Delta S$  would vary with

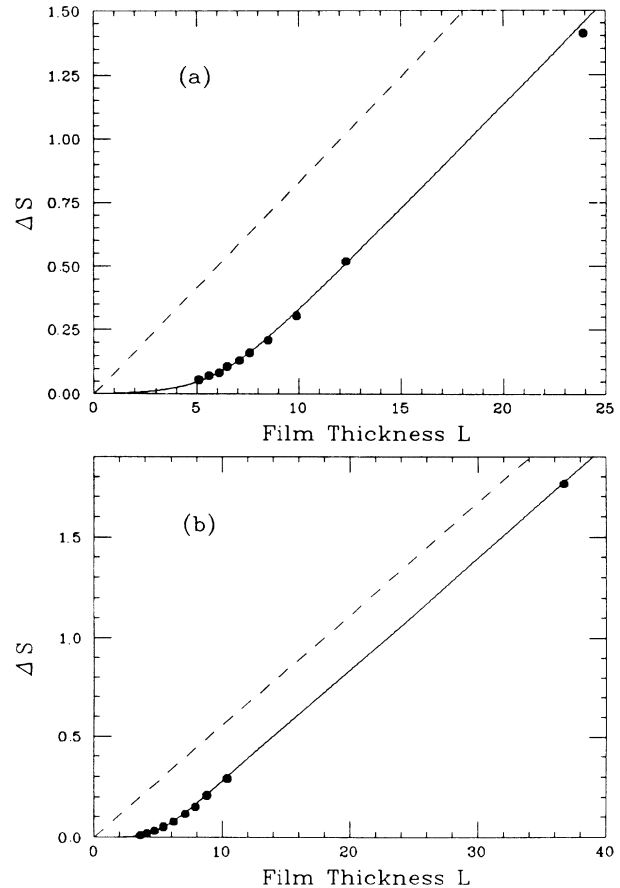


FIG. 4. Total entropy in the melting peaks of (a) Ne and (b) Ar films as functions of thickness. The broken lines correspond to the melting of equivalent quantities of bulk material, i.e., without surface corrections. The solid lines include calculated effects due to the finite width of the crystal-melt interface, and show the suppression of the total melting entropy due to the intrusion of solid order in the liquid adjacent to the solid boundary.

$L$  if there were no interfacial effects. The measured  $\Delta S(L)$  at large  $L$  tends to parallel the bulk lines but is shifted: The shift is approximately 7 layers in Ne and 5 layers in Ar. The shifts are due to a combination of substrate and crystal-melt interface effects. The cusp-shaped peak above the main anomaly in Fig. 1 is attributed to the melting of one substrate-field compressed layer; added evidence for compression is that the cusp contains only 0.2–0.3 of the transition entropy of an equal amount of bulk. Thus  $\Delta S(L)$  from the main anomaly is due to the melting of  $L-1$  layers. The remaining suppression is associated with the interface width; hence the width is about 6 layers in Ne and 4 layers in Ar.

The experimental widths are comparable to theoretical estimates and computer simulations.<sup>11–13</sup> However, the difference between the Ne and Ar values is unexpected in view of the similarities of the two systems. The difference is well outside of statistical uncertainty and seems unrelated to the details of the assumed interface profile function: A fit by the simple exponential form yields the same ratio of empirical correlation lengths. The exponential decay of the solid order parameter is the source of short-range effective interaction,<sup>4</sup> causing a logarithmic  $T$  dependence in thin films.

In conclusion, we point out that the method of integral analysis can be applied with experimental techniques other than calorimetry to explore additional properties of the crystal-melt interface. It should be possible to improve the resolution in future measurements in order to test some of the assumptions of the model, and to determine the actual profile of an interface.

We thank G. Gompper, R. E. Peierls, M. Schick, E. A. Stern, and O. E. Vilches for many helpful discus-

sions. This work is supported by National Science Foundation Grant No. DMR 86-11466.

<sup>1</sup>J. W. M. Frenken and J. F. van der Veen, Phys. Rev. Lett. **54**, 134 (1985); J. W. M. Frenken, P. M. Maree, and J. F. van der Veen, Phys. Rev. B **34**, 7506 (1986).

<sup>2</sup>R. H. Willens, A. Kornblit, L. R. Testardi, and S. Nakahara, Phys. Rev. B **25**, 290 (1982); G. Devaud and R. H. Willens, Phys. Rev. Lett. **57**, 2683 (1986).

<sup>3</sup>Da-Ming Zhu and J. G. Dash, Phys. Rev. Lett. **57**, 2959 (1986).

<sup>4</sup>R. Lipowsky, Phys. Rev. Lett. **49**, 1575 (1982); R. Lipowsky and W. Speth, Phys. Rev. B **28**, 3982 (1983).

<sup>5</sup>J. Q. Broughton and G. H. Gilmer, Acta Metall. **31**, 31 (1983).

<sup>6</sup>A. Trayanov and E. Tosatti, Phys. Rev. Lett. **59**, 2207 (1987).

<sup>7</sup>N. H. March, in *Physics of Simple Liquids*, edited by H. N. V. Temperley, J. S. Rowlinson, and G. S. Rushbrooke (Wiley Interscience, New York, 1969), p. 645.

<sup>8</sup>J. Krim, J. P. Coulomb, and J. Bouzidi, Phys. Rev. Lett. **58**, 583 (1987); R. Chiarello, J. P. Coulomb, J. Krim, and C. L. Wang, private communication.

<sup>9</sup>M. Bienfait, Europhys. Lett. **4**, 79 (1987).

<sup>10</sup>A. Bonissent, in *Interfacial Aspects of Phase Transitions*, edited by B. Mutaftschiev (Reidel, Dordrecht, 1982), pp. 143–182.

<sup>11</sup>J. W. Broughton, A. Bonissent, and F. F. Abraham, J. Chem. Phys. **74**, 7029 (1981).

<sup>12</sup>P. Tarazona and L. Vicente, Mol. Phys. **56**, 557 (1985).

<sup>13</sup>W. A. Curtin, Phys. Rev. Lett. **59**, 1228 (1987).

<sup>14</sup>R. K. Crawford, in *Rare Gas Solids*, edited by M. L. Klein and J. A. Venables (Academic, New York, 1977), Vol. 2, p. 664.

<sup>15</sup>J. Zittartz, Phys. Rev. **154**, 529 (1967).